

The Electronic Factor in Alkane Oxidation Catalysis

Maik Eichelbaum,^{*,†,‡} Michael Hävecker,^{†,¶} Christian Heine,[†] Anna Maria Wernbacher,[†] Frank Rosowski,^{‡,§} Annette Trunschke,[†] and Robert Schlögl[†]

[†]*Department of Inorganic Chemistry, Fritz-Haber-Institut der Max-Planck-Gesellschaft, Faradayweg 4-6, 14195 Berlin, Germany,* [‡]*BasCat, UniCat BASF JointLab, TU Berlin, Marchstraße 6, 10587 Berlin, Germany,* [¶]*Helmholtz Centre Berlin / BESSY II, Solar Energy Research, Albert-Einstein-Straße 15, 12489 Berlin, Germany,* and [§]*Process Research and Chemical Engineering, Heterogeneous Catalysis, BASF SE, Carl-Bosch-Straße 38, 67056 Ludwigshafen, Germany*

E-mail: me@fhi-berlin.mpg.de

Phone: +49 (0)30 84134566. Fax: +49 (0)30 84134405

Abstract

1
2 We are addressing the fundamental question, if semiconductor physics concepts can
3 be applied to describe the working mode of heterogeneous oxidation catalysts and if
4 they can be even used to discriminate between selective and unselective reaction path-
5 ways. By the application of near-ambient pressure X-ray photoelectron spectroscopy
6 it could be shown exemplarily for the oxidation of n-butane to maleic anhydride on the

*To whom correspondence should be addressed

[†]Fritz-Haber-Institut

[‡]BasCat, UniCat BASF JointLab

[¶]Helmholtz Centre Berlin / BESSY II

[§]BASF SE

7 highly selective catalyst vanadyl pyrophosphate and the moderately selective MoVTaN-
8 bOx M1 phase that the catalysts act like semiconducting gas sensors with a dynamic
9 bulk-surface charge transfer, as indicated by the gas phase response of the work func-
10 tion, electron affinity and the surface potential barrier. In contrast, only a minor
11 influence of the gas phase on the semiconducting properties and hence no dynamic
12 surface potential barrier was monitored for the total oxidation catalyst V_2O_5 . The
13 surface potential barrier is hence suggested as descriptor for selectivity.

14 Since the middle of the last century, semiconductor physics concepts have been used to
15 explain the working mode of selective alkane and alkene oxidation catalysts.¹⁻⁷ The vision
16 was - and still is - to predict the catalytic activity and selectivity of materials in different
17 reactions on the basis of their electronic structure (the so-called "electronic factor"). In semi-
18 conductor theory the difference between the Fermi potential of the semiconducting catalyst
19 and the redox potential of adsorbates creates a driving force for charge transfer across the
20 bulk-surface-adsorbate interface.^{5,8} This charge transfer generates a potential gradient and
21 hence electric field between surface and bulk and can induce conductive channels with cur-
22 rent rectifying properties like in a p-n junction diode.⁹ The height of this surface potential
23 barrier, which charge carriers have to overcome to move between bulk and surface, could
24 have a significant kinetic impact on the oxidation reaction on the surface and the activation
25 of oxygen.⁵ The surface barrier height under steady-state reaction conditions could hence be
26 a descriptor for the catalytic performance of oxidation catalysts. However, it has not proven
27 so far that oxidation catalysts act indeed like semiconducting gas sensors with the formation
28 of a surface potential barrier controlled by the gas phase.

29 Understanding the working mode of vanadyl pyrophosphate (VPP), which is the com-
30 mercial catalyst for the oxidation of n-butane to maleic anhydride.¹⁰⁻¹⁴ is of general interest,
31 since it is a benchmark system in selective oxidation catalysis,¹⁵⁻²¹ representing one of the
32 most important class of heterogeneously catalyzed reactions in context of the dawning raw
33 material change.²² Due to the increasing conductivity in air and decreasing conductivity in

34 n-butane containing gas mixtures, VPP was identified as p-type semiconductor with electron
35 holes as majority charge carriers.^{10-14,23-26} However, the conductivity response alone is not
36 a sufficient descriptor for selectivity, since vanadium(V) oxide exhibits as well a reversible
37 conductivity response under reaction conditions,²⁷ but catalyzes only the total oxidation of
38 n-butane to CO and CO₂.

39 In our contribution we report on the successful application of near-ambient pressure X-ray
40 photoelectron spectroscopy (NAP-XPS) to investigate the influence of the reactive gas phase
41 on the surface potential barrier of VPP under catalytic n-butane oxidation conditions with
42 proven maleic anhydride production. The results show that the transfer of charge carriers
43 between the bulk catalyst and the surface can be explained by - and are thus the first experi-
44 mental proof for - the previously only theoretically proposed semiconductor catalyst concepts
45 of Boudart,¹ Schwab,² Volkenshtein,³ and Morrison.^{4,5} We compare these results with the
46 electronic response of the unselective oxidation catalyst V₂O₅ and the moderately selective
47 catalyst MoVTaNbO_x (orthorhombic M1 phase) in order to identify a general concept that
48 can explain selectivity.

49 We investigated the polycrystalline catalyst VPP with NAP-XPS at 25 Pa and 400°C
50 in 1:10 n-butane/oxygen (C₄H₁₀/O₂), 1:10 helium/oxygen (O₂) and 1:10 n-butane/helium
51 (C₄H₁₀) mixtures, according to the protocol described in the Supporting Information. The
52 studied catalyst produces in a fixed-bed flow-through reactor at 1 bar maleic anhydride with
53 a selectivity between 70 and 80%.^{24,25} In semiconductor physics, a gas-phase dependent
54 surface potential barrier (band bending) and hence a charge carrier exchange between bulk
55 and surface can be evidenced, if the work function, the valence band and all core level binding
56 energies are consistently shifted by the same absolute value upon adsorbing different gases
57 (cf. Figure S2, in the Supporting Information).⁸ Thus, we measured the dependence of the
58 valence band onset, V3d valence state, work function (by measuring the secondary electron
59 cutoff), as well as of the O1s, V2p, and P2p core levels on the different gas mixtures. Figure 1
60 shows XP spectra at high (secondary electron cutoff) and low binding energies (valence band)

61 in the three different gas atmospheres. The peak close to the valence band at about 2-2.5 eV
62 below the Fermi level (0 eV) is assigned to an occupied vanadium 3d state. Upon changing
63 the applied gas mixture, the secondary electron cutoff, valence band onset, and V3d state
64 shift to higher binding energies under reducing C₄H₁₀ conditions, while only slight differences
65 can be recognized between spectra recorded in C₄H₁₀/O₂ and O₂ (Figure 1). Moreover, the
66 peak intensity of the V3d state increases under C₄H₁₀ conditions, indicating a larger electron
67 occupation of this valence state and hence reduction of the catalyst phase.

68 Figure 2 summarizes the observed changes of the work function, V3d state, vanadium oxida-
69 tion state (deduced from V2p_{3/2} core level) and electron affinity. The binding energy shifts
70 of the core levels V2p_{3/2}, O1s, and P2p are depicted in Figure S1 (Supporting Information).
71 The V3d state is reversibly shifted by up to 540 meV, while the measured core levels are
72 reversibly shifted by about 500 meV between oxidizing O₂ and reducing C₄H₁₀ conditions.
73 This consistent behavior is a strong indication for a bulk-surface charge transfer accom-
74 panied by the formation of a sub-surface space charge region and a gas-phase dependent
75 surface potential barrier (i.e. band bending). The proton-transfer reaction mass spectrom-
76 etry (PTR-MS) signal at m/z=99 (mass of protonated maleic anhydride), recorded during
77 the applied experimental protocol, proves that under C₄H₁₀/O₂ reaction conditions maleic
78 anhydride is produced and that the catalyst was indeed studied under catalytic operation
79 conditions (Figure 2a).

80 The work function Φ is deduced by calculating the difference between the excitation
81 energy and the energy value at half maximum of the secondary electron cutoff. The measured
82 work functions for VPP range between 6.94 eV in O₂ and 6.7 eV in C₄H₁₀ (Figure 2b).
83 These values are very well comparable with the work function of the binary oxide V₂O₅
84 ($\phi = 7.0$ eV).²⁸ As mentioned earlier, a pure Fermi level pinning to the adsorbate induced
85 surface states energy can be evidenced, if the work function and all valence and core level
86 binding energies are consistently shifted by the same absolute value upon adsorbing different
87 gases. However, the total changes of Φ are with up to 240 meV significantly smaller than

88 observed for the valence and core levels. Adsorbates on a surface of a semiconductor cannot
 89 only induce surface states causing band bending, but they can also affect the surface dipolar
 90 structure,⁸ which would be indicated by a modified surface electron affinity (Figure S2, in
 91 the Supporting Information). Since the energy shifts in the different gas mixtures between
 92 work function and valence/core level binding energies are different, the adsorbates have
 93 modified both surface dipoles and surface states.⁸ Thus, from this energy shift difference
 94 the electron affinity change $\Delta\chi$ induced by the adsorbates can be calculated (Figure 2e).
 95 Moreover, the average vanadium oxidation state is with nearly 4.4 highest in O₂, and with 4.0
 96 lowest in C₄H₁₀ (Figure 2d). Since the core level spectra were measured at a kinetic energy
 97 corresponding to a mean free electron path of 0.7 nm and hence comprehend basically the
 98 very first surface layer(s), the surface of VPP is obviously oxidized under O₂ and C₄H₁₀/O₂
 99 conditions in comparison to the VPP bulk vanadium oxidation state of 4.0.

100 The obtained results for the electronic response of VPP in the different gas mixtures are
 101 schematically summarized in a simplified band diagram (Figure 3). Notably, the electronic
 102 structure of the catalyst has not necessarily to be described by delocalized bands. If Fermi-
 103 Dirac electron statistics can be applied and electron or electron hole conduction can be
 104 described by a hopping mechanism of charge carriers between localized molecular orbitals, a
 105 similar double layer formation with an electric field between surface and bulk will form and
 106 similar binding energy shifts of the valence and core levels can be expected.

107 Band bending and the surface potential barrier are induced by the pinning of the Fermi
 108 potential to the surface state potential, being modified by the gas phase chemical potential.
 109 The surface states could be identified by a V⁴⁺/V⁵⁺ redox couple on the surface. In this
 110 case, the Fermi level (E_F) pinning is given by:⁵

$$E_F(\text{with surface states}) = E_t + kT \ln \frac{[V^{4+}]}{[V^{5+}]} \quad (1)$$

111 E_t could be approximated by the redox potential of the V^{4+}/V^{5+} couple. The suggested
112 relationship between surface barrier (band bending) and vanadium oxidation state is strongly
113 supported by the simultaneously observed modulation of the average vanadium oxidation
114 state (Figure 2d) and intensity of the V3d valence state (Figure 1). The surface potential
115 barrier height qV_B is the difference between the (hypothetical) Fermi level of the catalyst
116 without surface states and the Fermi level of the catalyst with surface states modified by the
117 gas phase as defined in eq 1:

$$qV_B = E_F(\text{without surface states, flatband}) - E_F(\text{with surface states}) \quad (2)$$

118 Many recent surface sensitive experiments under reaction conditions indicate that the
119 catalyst is terminated by a 2-dimensional vanadium(IV,V) oxide layer deviating significantly
120 from the bulk crystal structure.^{24,25,29-31} Hence, the proposed V^{4+}/V^{5+} surface states should
121 be a part of this termination layer, or in semiconductor physics nomenclature,⁵ are extrinsic
122 surface states from a surface termination with broken translational symmetry, as has been
123 already suggested by Boudart with his concept of a "defect one-phase surface system".¹

124 As indicated by eq 1 and eq 2, a high V^{5+}/V^{4+} ratio can increase the surface barrier
125 height qV_B to such values, that the bulk-surface electron transport is impeded. Under
126 such conditions, also the activation (reduction) of gas phase oxygen is strongly limited. As a
127 consequence, the surface barrier confines the concentration of activated oxygen on the surface.
128 Since an accumulation of oxygen will cause the total oxidation of the desired oxygenate to
129 CO_x , the surface potential barrier could control the catalytic selectivity.

130 In order to check the suggested relationship between surface barrier and selectivity, the
131 unselective (i.e. without selectivity to maleic anhydride, but only to CO and CO_2) catalyst
132 vanadium(V) oxide was investigated by NAP-XPS. Under strongly oxidizing conditions in
133 O_2 a maximum work function of 7.00 eV and a vanadium oxidation state of 4.9 is measured

134 (Figure 4a). A reduction to an average vanadium oxidation state of 4.8 is observed in
135 C_4H_{10} (Figure 4a). However, the work function is at the same time only slightly reduced
136 to 6.96 eV. Moreover, the valence band onset is only weakly changed from 2.18 eV (O_2)
137 to 2.22 eV (C_4H_{10}). Although all these changes are reversible and hence real, they are
138 much less pronounced than in VPP. As a consequence, the effect of the gases on the surface
139 barrier is small. This can be explained by the much higher conductivity of V_2O_5 ,²⁷ where
140 the depletion of electrons in the bulk by charge transfer between catalyst and gas phase is
141 negligible compared to its high charge carrier density. Hence, no surface potential barrier
142 due to a significant charge depletion in the sub-surface space charge region is formed or
143 modified. This has the consequence that the oxygen activation is not limited by the surface
144 barrier, which could indeed explain the observed total oxidation of n-butane to CO_x .

145 In addition, we investigated an alternative selective n-butane oxidation catalyst, the or-
146 thorhombic $MoVTeNbO_x$ M1 phase, with a maleic anhydride selectivity of more than 40%.³²
147 The gas phase conditions were shifted between 1:2 mixtures of ethane/ O_2 and n-butane/ O_2
148 to mimic a more oxidizing and reducing atmosphere, respectively, since the catalyst is not
149 stable in pure O_2 or n-butane at reduced pressures. The vanadium oxidation state changed
150 (reversibly) from about 4.6 to 4.5 (oxidation states of the other metal ions remained con-
151 stant³²), the work function shifted by 200 meV and the valence band onset by about 70 meV
152 (Figure 4b), indicating a gas-phase dependent surface potential barrier and a change of the
153 surface electron affinity by about 130 meV. Since the shifts are significantly larger than
154 observed for V_2O_5 , despite the milder changes in the oxidation/reduction conditions, these
155 results are in line with the intermediate selectivity of this catalyst and support the concept of
156 a surface barrier mediated bulk-surface charge transfer influencing the catalytic selectivity.
157 The strong surface restructuring indicated by the electron affinity change observed for both
158 selective catalysts is in line with the idea that the active surface is formed in the presence
159 of reaction gases as generally observed in selective alkane oxidation catalysis.³³

160 In conclusion, NAP-XPS experiments prove that the selective alkane oxidation catalysts

161 VPP and MoVTeNbO_x M1 phase act like semiconducting gas sensors with a gas phase
162 dependent surface potential barrier. These results can hence be considered as an exper-
163 imental proof for the early semiconductor catalyst concepts of Boudart,¹ Schwab,² and
164 Volkenshtein.³ The formation of a dynamic surface potential barrier could give a rational
165 description for catalytic selectivity in oxidation reactions. Within this concept the surface
166 barrier controls the transfer of charge carriers between bulk and surface, and hence the ac-
167 tivation of oxygen on the surface. This interpretation is strongly supported by experiments
168 on the unselective catalyst V₂O₅, where the effect of the gas phase on the surface potential
169 barrier was minute.

170 **Acknowledgement**

171 The work was conducted in the framework of the BasCat collaboration between BASF SE,
172 TU Berlin, FHI and the cluster of excellence Unicat. The HZB staff is acknowledged for
173 their continual support of the electron spectroscopy activities of the FHI at BESSY II.

174 **References**

- 175 (1) Boudart, M. *J. Am. Chem. Soc.* **1952**, *74*, 1531–1535.
- 176 (2) Schwab, G.-M. *Angew. Chem.* **1961**, *73*, 399–401.
- 177 (3) Volkenshtein, F. F. *The Electronic Theory of Catalysis on Semiconductors*; Pergamon
178 Press, 1963.
- 179 (4) Morrison, S. R. *J. Catal.* **1974**, *34*, 462–478.
- 180 (5) Morrison, S. R. *The Chemical Physics of Surfaces*; Plenum Press, 1977.
- 181 (6) Haber, J.; Witko, M. *J. Catal.* **2003**, *216*, 416–424.
- 182 (7) Herrmann, J. M. *Catal. Today* **2006**, *112*, 73–77.

- 183 (8) Mönch, W. *J. Vac. Sci. Technol. B* **1989**, *7*, 1216–1225.
- 184 (9) Lüth, H. *Space Charge Layer*; Springer Verlag, 2001; Chapter Electronic structure of
185 Surfaces, pp 329 – 380.
- 186 (10) Rouvet, F.; Herrmann, J. M.; Volta, J. C. *J. Chem. Soc. Faraday Trans.* **1994**, *90*,
187 1441–1448.
- 188 (11) Herrmann, J. M.; Vernoux, P.; Bere, K. E.; Abon, M. *J. Catal.* **1997**, *167*, 106–117.
- 189 (12) Ait-Lachgar, K.; Tuel, A.; Brun, M.; Herrmann, J. M.; Krafft, J. M.; Martin, J. R.;
190 Volta, J. C.; Abon, M. *J. Catal.* **1998**, *177*, 224–230.
- 191 (13) Rihko-Struckmann, L. K.; Ye, Y.; Chalakov, L.; Suchorski, Y.; Weiss, H.; Sund-
192 macher, K. *Catal. Lett.* **2006**, *109*, 89–96.
- 193 (14) Sartoni, L.; Delimitis, A.; Bartley, J. K.; Burrows, A.; Roussel, H.; Herrmann, J. M.;
194 Volta, J. C.; Kiely, C. J.; Hutchings, G. J. *J. Mater. Chem.* **2006**, *16*, 4348–4360.
- 195 (15) Centi, G.; Trifiro, F.; Ebner, J. R.; Franchetti, V. M. *Chem. Rev.* **1988**, *88*, 55–80.
- 196 (16) Centi, G. *Catal. Today* **1993**, *16*, 5–26.
- 197 (17) Volta, J. C. *Comptes Rendus De L Academie Des Sciences Serie Ii Fascicule C-chimie*
198 **2000**, *3*, 717–723.
- 199 (18) Grasselli, R. K. *Top. Catal.* **2001**, *15*, 93–101.
- 200 (19) Ballarini, N.; Cavani, F.; Cortelli, C.; Ligi, S.; Pierelli, F.; Trifiro, F.; Fumagalli, C.;
201 Mazzoni, G.; Monti, T. *Top. Catal.* **2006**, *38*, 147–156.
- 202 (20) Dummer, N. F.; Bartley, J. K.; Hutchings, G. J. *Adv. Catal.* **2011**, *54*, 189–247.
- 203 (21) Védrine, J. C.; Hutchings, G. J.; Kiely, C. J. *Catal. Today* **2013**, *217*, 57–64.
- 204 (22) Cavani, F. *Catal. Today* **2010**, *157*, 8–15.

- 205 (23) Eichelbaum, M.; Stößer, R.; Karpov, A.; Dobner, C.-K.; Rosowski, F.; Trunschke, A.;
206 Schlögl, R. *Phys. Chem. Chem. Phys.* **2012**, *14*, 1302–1312.
- 207 (24) Eichelbaum, M.; Hävecker, M.; Heine, C.; Karpov, A.; Dobner, C. K.; Rosowski, F.;
208 Trunschke, A.; Schlögl, R. *Angew. Chem. Int. Ed.* **2012**, *51*, 6246–6250.
- 209 (25) Eichelbaum, M.; Hävecker, M.; Heine, C.; Karpov, A.; Dobner, C. K.; Rosowski, F.;
210 Trunschke, A.; Schlögl, R. *Angew. Chem.* **2012**, *124*, 6350–6354.
- 211 (26) Eichelbaum, M.; Glaum, R.; Hävecker, M.; Wittich, K.; Heine, C.; Schwarz, H.; Dob-
212 ner, C. K.; Welker-Nieuwoudt, C.; Trunschke, A.; Schlögl, R. *ChemCatChem* **2013**, *5*,
213 2318–2329.
- 214 (27) Heine, C.; Girgsdies, F.; Trunschke, A.; Schlögl, R.; Eichelbaum, M. *Appl. Phys. A:*
215 *Mater. Sci. Process.* **2013**, *112*, 289–296.
- 216 (28) Meyer, J.; Zilberberg, K.; Riedl, T.; Kahn, A. *J. Appl. Phys.* **2011**, *110*, 033710.
- 217 (29) Kleimenov, E.; Bluhm, H.; Hävecker, M.; Knop-Gericke, A.; Pestryakov, A.;
218 Teschner, D.; Lopez-Sanchez, J. A.; Bartley, J. K.; Hutchings, G. J.; Schlögl, R. *Surf.*
219 *Sci.* **2005**, *575*, 181–188.
- 220 (30) Hävecker, M.; Mayer, R. W.; Knop-Gericke, A.; Bluhm, H.; Kleimenov, E.;
221 Liskowski, A.; Su, D.; Follath, R.; Requejo, F. G.; Ogletree, D. F.; Salmeron, M.;
222 Lopez-Sanchez, J. A.; Bartley, J. K.; Hutchings, G. J.; Schlögl, R. *J. Phys. Chem. B*
223 **2003**, *107*, 4587–4596.
- 224 (31) Bluhm, H.; Hävecker, M.; Kleimenov, E.; Knop-Gericke, A.; Liskowski, A.; Schlögl, R.;
225 Su, D. S. *Top. Catal.* **2003**, *23*, 99–107.
- 226 (32) Heine, C.; Hävecker, M.; Sanchez-Sanchez, M.; Trunschke, A.; Schlögl, R.; Eichel-
227 baum, M. . *J. Phys. Chem. C* **2013**, *117*, 26988–26997.
- 228 (33) Schlögl, R. *Top. Catal.* **2011**, *54*, 627–638.

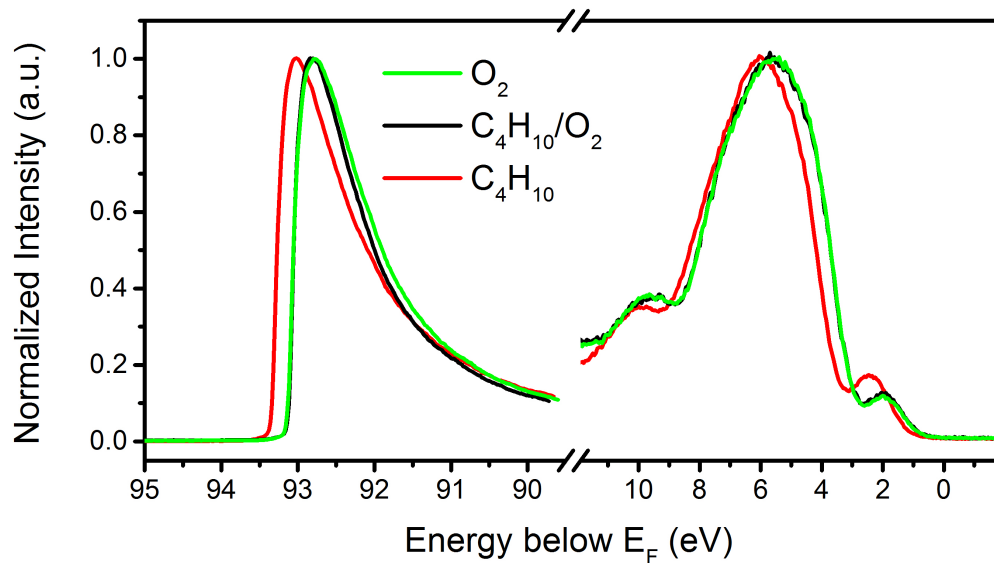


Figure 1: High (secondary electron cutoff; left) and low binding energy edge (valence band with V3d state at about 2 eV; right) of the XP spectra of VPP at 400°C under catalytic working (C_4H_{10}/O_2), oxidizing (O_2) and reducing conditions (C_4H_{10}), respectively. The spectra were measured with an excitation energy of 100 eV.

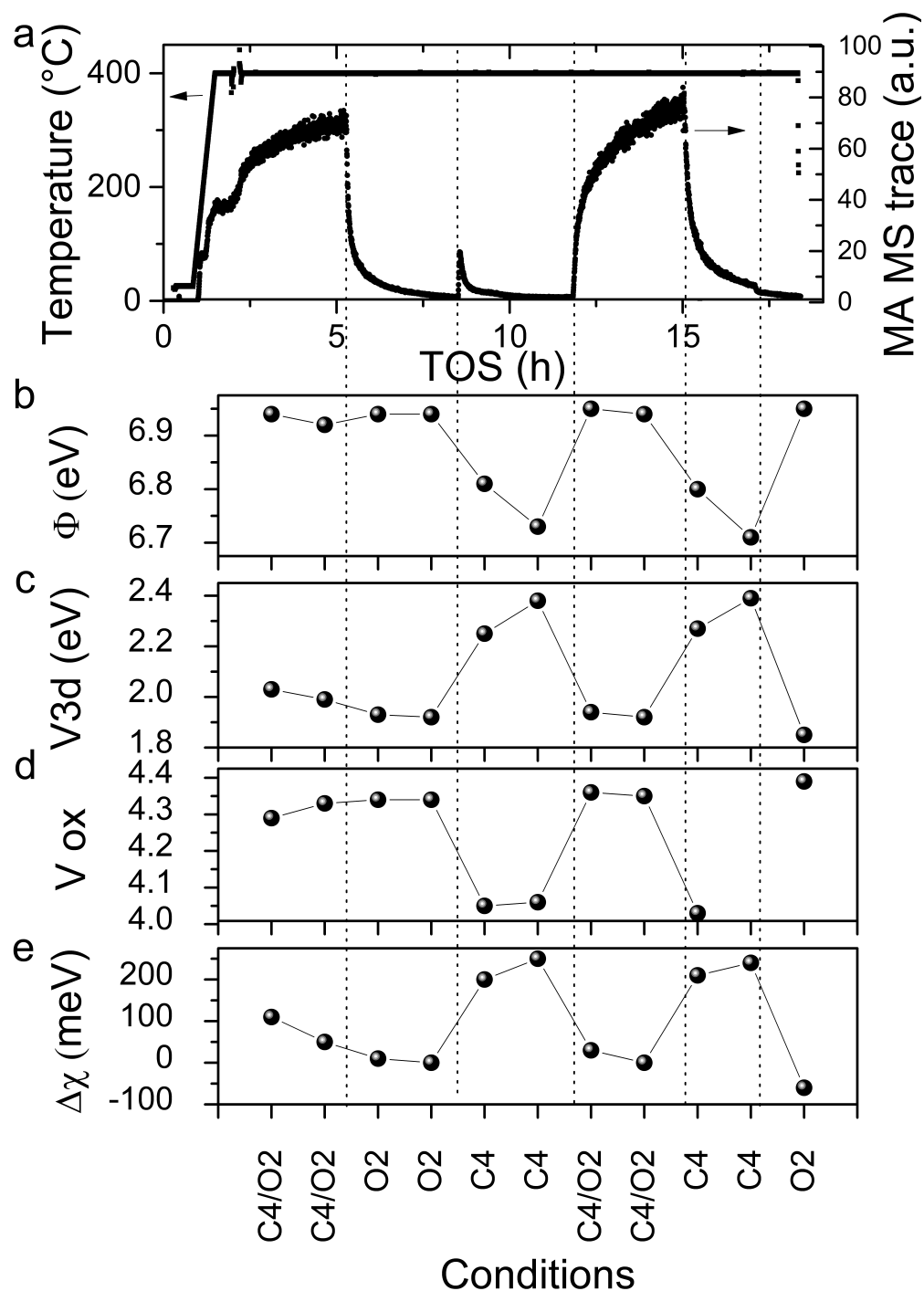


Figure 2: a) PTR-MS trace of maleic anhydride (MA; protonated mass 99) during time on stream (TOS) under conditions indicated in the abscissa of e, b) work function Φ , c) V3d valence state binding energy, d) average vanadium oxidation state (V ox) as deduced from the V2p_{3/2} spectra, and e) electron affinity change $\Delta\chi$ ($\Delta\Phi - \Delta\text{BE}(\text{V3d})$, difference to 2nd O₂ condition) of VPP at 400°C in different gas mixtures.

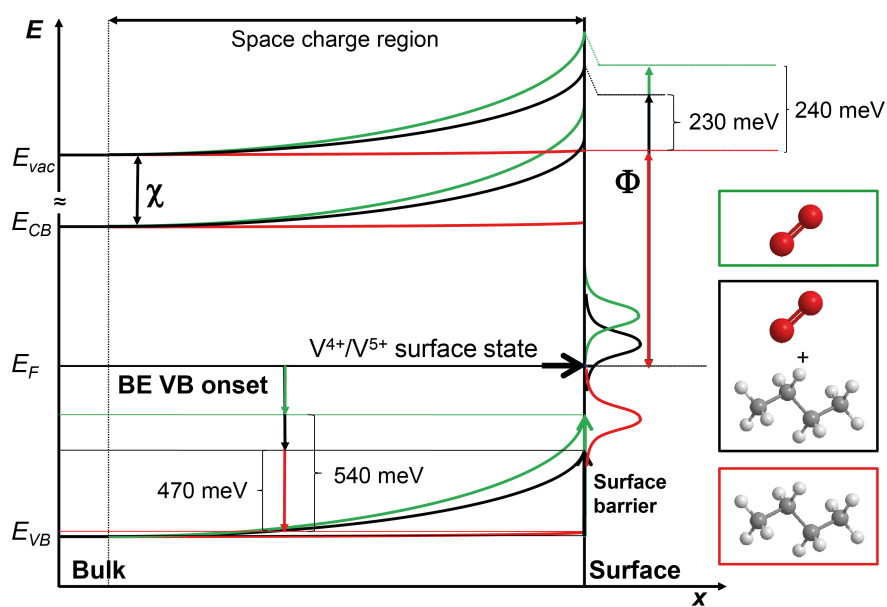


Figure 3: Schematic band diagram of VPP with experimentally obtained values for the binding energy (BE) shifts of the valence band (VB) onset and of the work function Φ measured in n-butane/helium (red), n-butane/oxygen (black), oxygen/helium (green). E_{VB} : valence band onset, E_F : Fermi level, E_{CB} : conduction band minimum, E_{vac} : vacuum level, χ : electron affinity.

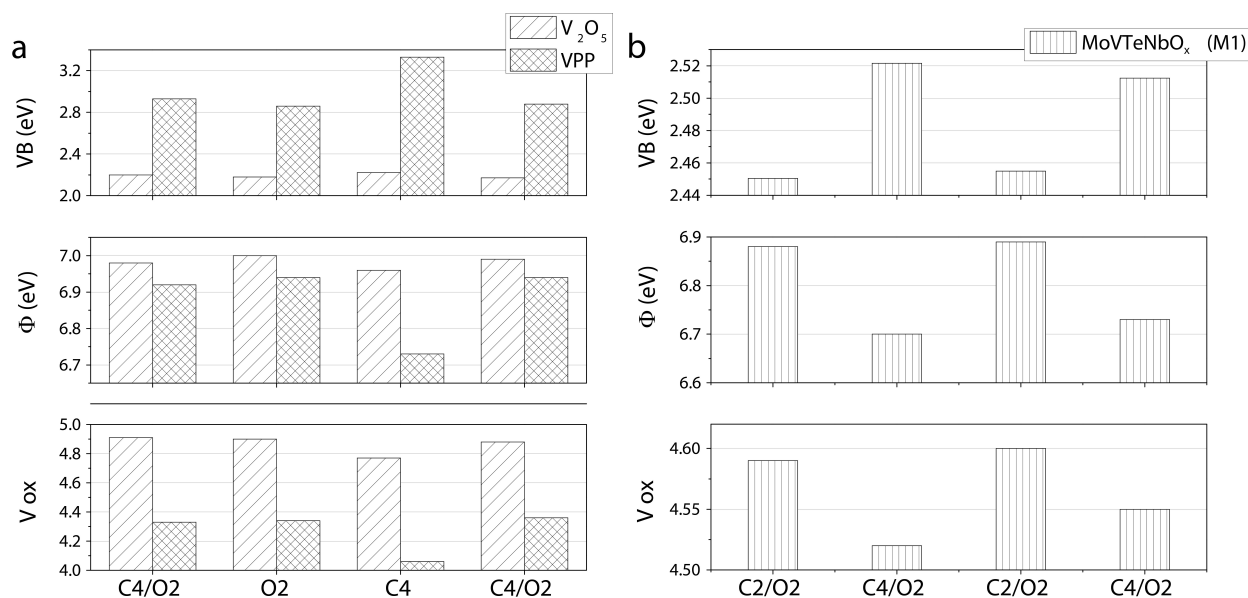


Figure 4: Valence band onset (VB), work function Φ , and surface vanadium oxidation state (V ox) of VPP, V₂O₅ (a) and MoVTeNbO_x M1 phase (b) at 400°C in different gas mixtures.